nature neuroscience

Structural basis for modulation of Kv4 K^+ channels by auxiliary KChIP subunits

Huayi Wang[1,4], Yan Yan[2,4], Qun Liu[3], Yanhua Huang[2], Yue Shen[1], Linjie Chen[1], Yi Chen[2], Qiuyue Yang[3], Quan Hao[3], KeWei Wang[2] & Jijie Chai[1]

KChIPs coassemble with pore-forming Kv4 α subunits to form a native complex in the brain and heart and regulate the expression and gating properties of Kv4 K^+ channels, but the mechanisms underlying these processes are unknown. Here we report a co-crystal structure of the complex of human Kv4.3 N-terminus and KChIP1 at a 3.2-Å resolution. The structure reveals a unique clamping action of the complex, in which a single KChIP1 molecule, as a monomer, laterally clamps two neighboring Kv4.3 N-termini in a 4:4 manner, forming an octamer. The proximal N-terminal peptide of Kv4.3 is sequestered by its binding to an elongated groove on the surface of KChIP1, which is indispensable for the modulation of Kv4.3 by KChIP1, and the same KChIP1 molecule binds to an adjacent T1 domain to stabilize the tetrameric Kv4.3 channels. Taken together with biochemical and functional data, our findings provide a structural basis for the modulation of Kv4 by KChIPs.

A native complex of voltage-gated potassium channels (Kv) is composed of a tetrameric core of pore-forming α-subunits and additional auxiliary subunits. Binding of auxiliary subunits can change the functional properties of Kv channels at the membrane surface, as well as their intracellular trafficking and gating kinetics[1–5]. Cytosolic Kv channel-interacting proteins (KChIPs, which are ~217–256 amino acids in size), which belong to the neuronal calcium sensor family of calcium binding EF-hand proteins, coassemble with Kv4 (also known as Shal) α-subunits to form a native complex that encodes the somatodendritic A-type K^+ current, I_{SA}, in neurons and the transient outward current, I_{TO}, in cardiac myocytes[6–9]. The A-type K^+ current is important in regulating neuronal excitability, by shaping the action potential, because of its characteristic kinetics of fast inactivation, recovery from inactivation and somatodendritic localization in neurons[10–16].

The specific binding of KChIPs to the Kv4 N-terminus enhances surface expression, facilitates subunit assembly and regulates the functional gating properties of Kv4 channels[3,6,8,17]. The enhancement of channel expression by KChIPs has been attributed to their trafficking effects, as a result of protein redistribution to the cell surface, although the exact mechanism is not known[3]. The structure of the Kv4 N-terminus contains the intersubunit Zn^{2+} binding sites in the cytoplasmic N-terminal portion known as the tetramerization, or T1, domain that is highly conserved among Kv channels[18–20]. Mutations affecting the Zn^{2+} binding site that disrupt the interactions of the T1 domain can trap the protein in the endoplasmic reticulum and shift the gel migration of tetrameric subunits to monomeric molecular weights[17]. It has been shown that KChIPs are capable of rescuing the function of Zn^{2+} binding site mutations by driving the mutant subunits to form tetramers and by stabilizing the tetrameric assembly[17]. In addition to increasing expression and facilitating tetramerization, KChIPs cause substantial changes in the channel gating properties by drastically slowing inactivation and by hastening recovery from inactivation[8].

Structural efforts, combined with mutagenesis and electrophysiological assays, from several studies have recently attempted to address the underlying mechanism of interaction between Kv4 and KChIPs[19,21,22]. The crystal structure of KChIP1 reveals that it can be divided into N- and C-terminal lobes, with two Ca^{2+} ions mapped to the last two of the four EF hands (EF-3 and EF-4)[19,21]. Five α-helices (H1–H5) are located in the hydrophilic N-terminal lobe and helices H6–H10 form the hydrophobic C-terminal lobe[19]. Because of the bipolar nature of KChIP1, we previously proposed that the hydrophobic proximal N-terminus of Kv4 may interact with the hydrophobic surface of KChIP1 (ref. 19). By creating a tandem complex of KChIP1 with the first 30 N-terminal amino acids of Kv4.2, earlier researchers obtained the crystal structure of a clam-shaped dimeric assembly, with the first 20 residues of Kv4.2 collinear with KChIP1 in a head-to-tail fashion[21]. Intact, functional-quality Kv4.2-KChIP2 complexes were purified from mammalian cells and the three-dimensional structure of the channel complex was determined by electron microscopy (EM) at 21-Å resolution[22]. The EM structure reveals a 4:4 complex, in which KChIP2 forms four peripheral columns (offset by 45°) that appear to attach laterally to the four inner windows of the T1 gondola, suggesting a unique structural arrangement of Kv4.2-KChIP2, in contrast with the previously characterized T1-Kvβ2 complex in which Kvβ2 is located right below the gondola[23,24].

[1]National Institute of Biological Sciences, No. 7 Science Park Road, Beijing 102206, China. [2]Neuroscience Research Institute, Department of Neurobiology, Key Laboratory for Neuroscience of the Ministry of Education, Center for Protein Sciences, Peking University Health Science Center, 38 Xueyuan Road, Beijing 100083, China. [3]Cornell High-Energy Synchrotron Source, Cornell University, Ithaca, New York 14853, USA. [4]These authors contributed equally to this work. Correspondence should be addressed to K.W.W. (wangkw@bjmu.edu.cn) or J.C. (chaijijie@nibs.ac.cn).

Received 24 October; accepted 29 November; published online 24 December 2006; doi:10.1038/nn1822

Table 1 Data collection and statistics for refinement

Data collection	
Space group	*I*222
Resolution	99.0–3.2 Å
Data coverage (outer shell)	98.0% (98.7%)
Cell unit	$a = 112.186$ Å, $b = 112.213$ Å, $c = 41.051$ Å, $\alpha = \gamma = \beta = 90^\circ$
R_{sym} (outer shell)	6.2% (48.9%)
Redundancy	5.9
Refinement	
Resolution range (Å)	20.0–3.2
Number of reflections ($\|F\| > 0$)	13,510
$R_{working}$ / R_{free}	25.8% / 30.2%
Number of atoms:	
Protein	5,116
Ca^{2+}	4
Zn^{2+}	2
R.m.s. deviation bond length (Å)	0.007
R.m.s. deviation bond angles (°)	0.899

$R_{sym} = \Sigma_h\Sigma_i|I_{h,i} I_h|/\Sigma_h\Sigma_i I_{h,i}$, where I_h is the mean intensity of the i observations of symmetry-related reflections of h. $R = \Sigma||F_{obs}| |F_{calc}||/\Sigma|F_{obs}|$, where $F_{obs} = F_P$, and F_{calc} is the calculated protein structure factor from the atomic model. r.m.s. deviation in bond lengths and angles are the deviations from ideal values, and the r.m.s. deviation in *B* factors is calculated between bonded atoms.

Despite intensive efforts, the mechanisms by which KChIPs modulate Kv4 channels have remained elusive. In the present study, we explored the structural basis for the regulation of Kv4 channels by their auxiliary KChIP subunits. Here we report a co-crystal structure of a complex between the human Kv4.3 N-terminus (residues 6–145) and human KChIP1 (residues 38–217) at a 3.2-Å resolution. The structure reveals that one KChIP1 molecule binds to two neighboring Kv4.3 N-termini in a 4:4 manner, with two contact interfaces being involved in the interaction. The proximal N-terminal peptide of Kv4.3 is deeply buried within an elongated groove on the surface of KChIP1, in which the H10 helix of KChIP1 is replaced by the Kv4.3 N-terminal peptide, while the same KChIP1 molecule binds to another adjacent T1 domain through hydrophobic interactions and hydrogen bonds, resulting in a stabilized tetrameric Kv4.3 T1–KChIP1 complex. Electrophysiological assays, combined with biochemistry and mutagenesis, further confirmed that disruption of either of the two interfaces resulted in the loss of the KChIP1 effects on the modulation of channel gating kinetics and expression of Kv4.3.

RESULTS

Overall architecture of the complex

Coexpression of the human Kv4.3 N-terminus (residues 6–145, hereafter referred to as Kv4.3N) and human KChIP1 (residues 38–217) in BL21 (DE3) cells yielded a stable complex of the two proteins. The complex was purified to homogeneity and crystallized and its structure was determined by molecular replacement using the structures of the T1 domain of Kv4.3 and KChIP1 as the searching models[19]. The final model was refined to a crystallographic R_{factor} of 25.8% (R_{free} 30.2%) (**Table 1**). One asymmetric unit contains two KChIP1-Kv4.3N complexes from which a 4:4 complex can be generated through symmetric operations (**Fig. 1a**,**b**). Each KChIP1 monomer (as opposed to dimer) interacts with two adjacent Kv4.3Ns, 'clamping' them together, which results in two contact interfaces composed of one KChIP1 and two Kv4.3Ns (**Fig. 1c**,**d**). This provides evidence that the complex is not a dimeric assembly as has been suggested previously[21]. The proximal N-terminal hydrophobic peptide (residues 6–21, hereafter referred to as the N-terminal peptide) of Kv4.3 reaches out into a deep, elongated groove and is sequestered by binding to the deep hydrophobic pocket on the surface of KChIP1, forming the first interface in the complex (**Fig. 1c**, **Fig. 2**, and **Fig. 3**). In addition, the N-terminal peptide is further capped by its adjacent segment, residues 23–40. All of these conformational changes result in the immobilization of the Kv4.3 N-terminal peptide (**Fig. 3a**), preventing it from functioning as an inactivation peptide, although the exact mechanism of Kv4 inactivation is not fully understood[25–27]. More notably, the same KChIP1 molecule interacts with another Kv4.3N in the complex, resulting in a second contact interface (**Fig. 1c** and **Fig. 4**). This molecular clamp in which one KChIP1 molecule binds to two Kv4.3Ns simultaneously is propagated four times, thereby stabilizing the tetramerization of Kv4.3 channels (**Fig 1d**). Despite the clamping effects of KChIP1 on Kv4.3, the overall architecture of the tetrameric T1 domains of Kv4.3 remains unchanged compared with those in the protein's free form, with a root-mean-square (r.m.s.) deviation of 0.60 Å for all of the aligned Cα atoms of the 4 Kv4.3Ns (as discussed later).

The first interface is responsible for inactivation

The first contact interface consists of the Kv4.3 N-terminal peptide binding to a deep hydrophobic pocket on the surface of KChIP1, which demonstrates the physical suppression of Kv4 inactivation by KChIPs (**Fig. 2a**–**c**). Although the overall positioning of the Kv4.3 T1 domain

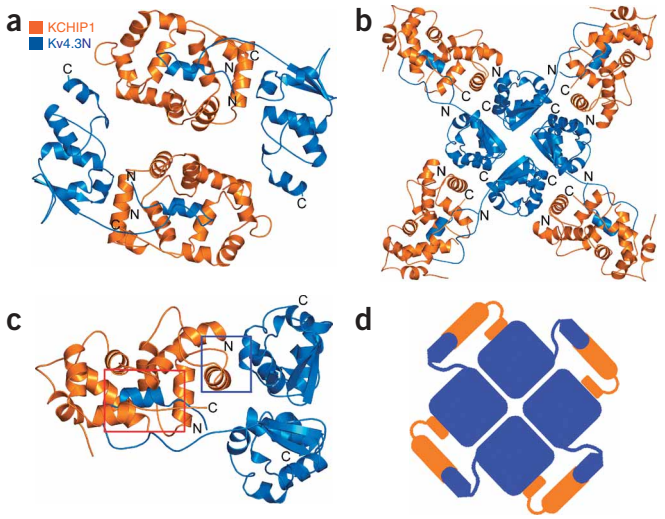

Figure 1 The overall architecture of the KChIP1–Kv4.3N complex. All panels have the same color codes, with some secondary structural elements labeled specifically. (**a**) Schematic representation of the complex structure in one asymmetric unit. Two KChIP1 and two Kv4.3 molecules are shown in orange and blue, respectively. (**b**) The 4:4 complex of KChIP1-Kv4.3N shown was generated from the complex in **a** through symmetric operations. The complex in this panel has the same size as the one shown in **Figure 6a**. (**c**) One KChIP1 molecule interacts simultaneously with two Kv4.3Ns. In the complex, each KChIP1 molecule not only binds to the N-terminal peptide of one Kv4.3 but also interacts with an adjacent Kv4.3 T1 domain, forming two contact interfaces; the first interface is shown in the red frame and second interface is shown in the blue frame. (**d**) A cartoon of the KChIP1-Kv4.3N complex in 4:4 showing the clamping effect of KChIP1 molecule on the tetramer of Kv4.3.

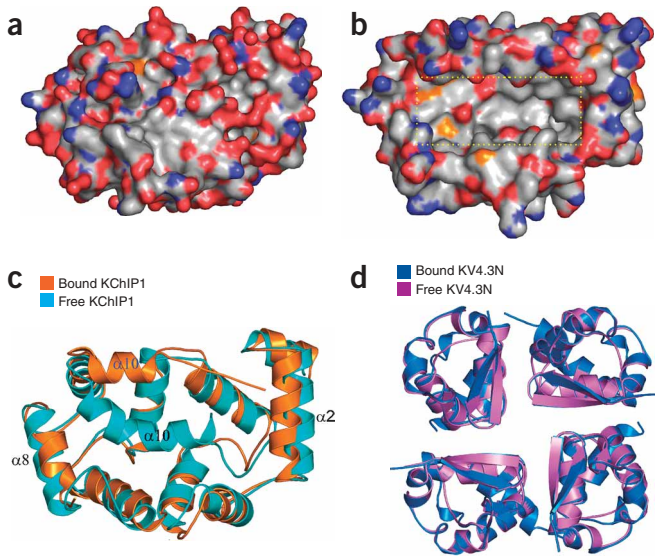

Figure 2 Significant structural rearrangements occur to KChIP1 upon Kv4.3 N-terminal binding. (**a**,**b**) Surface representations are shown for an isolated KChIP1 (**a**) and Kv4.3-bound KChIP1 (**b**). The two KChIP1 molecules are in the same orientation and can be aligned with each other with an r.m.s. deviation of 1.86 Å. The positive, negative and hydrophobic surfaces of KChIP1 are highlighted in red, blue and white, respectively. Note the striking hydrophobic groove indicated by yellow dashed dots on the Kv4.3-bound KChIP1, with a size of ~30 × 16 × 12 Å, depicted in **b**. (**c**) Structural alignment between the isolated KChIP1 (pink) and the Kv4.3-bound KChIP1 (blue). For clarity, the N-terminal peptide of Kv4.3 in the Kv4.3-bound KChIP1 is not shown. α helix 10 is labeled in red, rotating about 40° outward in the Kv4.3-bound KChIP1, whereas the helices α2 and α8 have translated 2.5 and 1.5 Å, respectively. (**d**) Tetrameric structures of free and bound Kv4.3N remain unchanged.

remained essentially unchanged after binding to KChIP1 (**Fig. 2d**), some regions of KChIP1 underwent significant structural rearrangements compared with the isolated KChIP1, as indicated by an r.m.s. deviation of 1.86 Å over all of the aligned Cα atoms (**Fig. 2c**). The most notable conformational change in the Kv4.3-bound KChIP1 occurs in H10, which is completely replaced by the N-terminal peptide of Kv4.3 and swings outward, ~40° from the hydrophobic groove (**Fig. 2c**). In addition, H2 and H8 have translated outward by ~2.5 Å and ~1.5 Å, respectively, further contributing to the configuration of the peptide binding pocket on the surface of KChIP1 (**Fig. 2c**). As a result, all of these structural changes create a clear-cut hydrophobic groove on the surface of KChIP1 (**Fig. 2b**) that is completely hidden in the free KChIP1 structure (**Fig. 2a**). It is noteworthy that the binding of Kv4.3N does not cause the relative rotations between the N- and C-terminal lobe of KChIP1, such as are observed in complexes composed of other EF-hand proteins and their target proteins[28].

The N-terminal peptide of Kv4.3 forms an α-helix that is followed by an extended segment and binds to the deep pocket of KChIP1. The interaction around this region is predominantly mediated by hydrophobic contacts. Almost all of the hydrophobic residues from the N-terminal peptide of Kv4.3 are involved in the extensive interactions with their neighboring residues from KChIP1, resulting in a burial of 2,352 Å^2 of exposed surface. Trp8 and Trp19, two highly conserved bulky residues among the Kv4 members (**Fig. 3c**), are positioned at both ends of the deep groove and can best be characterized as two pillars that support the whole peptide on the surface of KChIP1 (**Fig. 3a**). Trp19 contributes to the interaction between Kv4.3N and KChIP1 by docking in the deep hydrophobic groove and making van der Waals contacts with seven KChIP1 residues, Tyr134, Ile150, Val151, Tyr155, Ile154, Phe178 and the Cα atom of His174. On the N-terminus of the peptide, the two conserved bulky hydrophobic residues Trp8 and Phe11 are tightly fitted into another hydrophobic cavity that is built by nine KChIP1 residues, Ile77, Tyr78, Phe74, Leu94, Phe111, Leu115, Leu118, Phe60 and the Cα atom of Gly59. Although the orientation of the N-terminal peptide of Kv4.2 when it is fused to the C-terminus of KChIP1 is the reverse of that observed in the current structure[21], the position of Trp8 is almost identical in both structures (data not shown). To further strengthen the hydrophobic interaction, residues Leu9, Pro10, Ala12,

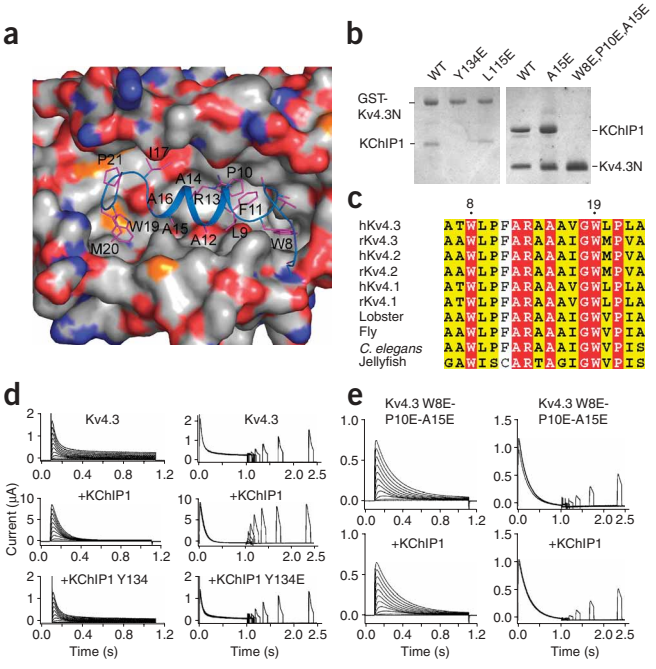

Figure 3 The N-terminal inactivation peptide of Kv4.3 is completely sequestered in a hydrophobic groove on the surface of KChIP1. (**a**) The N-terminal hydrophobic peptide of Kv4.3 binds to an elongated hydrophobic groove on the surface of KChIP1. KChIP1 is shown in the surface representation and the N-terminal inactivation peptide of Kv4.3 is shown as a ribbon. The Kv4.3 N-terminal residues that are involved in hydrophobic contacts with KChIP1 are colored in magenta. (**b**) An SDS-PAGE gel showing the pull-down results for the point mutants of both KChIP1 and the N-terminal peptide of Kv4.3. The single mutation of KChIP1 or (Y134E) and the triple mutation W8E, P10E and A15E of Kv4.3, completely abolished their interactions with their respective wild-type partners. A GST pull-down assay was used to detect the interaction between wild-type Kv4.3N and the KChIP1 mutants (left); various His-tagged Kv.3 mutants were immobilized on Ni resin and WT KChIP1 was allowed to flow through Ni resin (right). In both cases, the resin was visualized on SDS-PAGE followed by Coomassie staining. (**c**) Sequence alignments of the N-terminal peptide of Kv4-family proteins among different species. (**d**) Effects of KChIP mutations in the first interface on Kv4.3. The representative traces recorded from oocytes injected with cRNAs of wild-type Kv4.3 alone, wild-type Kv4.3 + wild-type KChIP1 and wild-type Kv4.3 + KChIP Y134E are depicted. Left, currents recorded from oocytes held at –80 mV by a family of pulses from –60 to 40 mV in 10 mV increments for 1 s; right, recovery from inactivation for varying lengths of time at step from –80 to 40 mV. (**e**) The representative traces of Kv4.3 triple mutant (W8E-P10E-A15E) alone and the triple mutant + wild-type KChIP1 recorded from oocytes under the same protocol as in **d**.

Table 2 Gating kinetics of Kv4.3 and mutants with and without coexpressed KChIP1 and mutants

	Current change (fold)	Inactivation τ_1 (ms, 40 mV)	Inactivation τ_2 (ms, 40 mV)	Recovery τ_{rec} (ms)
Kv4.3 WT	1.0	56.6 ± 3.9	281 ± 18.2	455.8 ± 24.1
Kv4.3 WT + KChIP1	8.1 ± 1.1*	84.0 ± 3.4*	121.5 ± 18.6*	161.7 ± 13.8*
Kv4.3 WT + KChIP1 Y134E	1.5 ± 0.3	41.9 ± 2.5	238.1 ± 23.8	324.3 ± 42.7
Kv4.3 W8E-P10E-A15E	1.0	106.7 ± 2.2	225.7 ± 7.1	628.6 ± 74.2
Kv4.3 W8E-P10E-A15E + KChIP1	0.91 ± 0.09	73.2 ± 26.2	207.5 ± 22.8	649.5 ± 82.7
Kv4.3 E70A-F73E	1.0	26.2 ± 1.5	158.7 ± 23.1	537.3 ± 52.8
Kv4.3 E70A-F73E + KChIP1	2.6 ± 0.4	44.2 ± 3.14*	136.1 ± 12.1	507.1 ± 40.0
Kv4.3 E70A-F73E + KChIP1 L39E-Y57A-K61A	0.9 ± 0.12	51.3 ± 6.4	194.2 ± 48.6	548.0 ± 48.6
Kv4.3 C110A	1.0	82.2 ± 3.5	282.5 ± 14.4	482.1 ± 26.8
Kv4.3 C110A + KChIP1	3.36 ± 0.22 *	273.2 ± 15.0*	273.9 ± 29.2	147.1 ± 12.6*
Kv4.3 C110A + KChIP1 L39E-Y57A-K61A	1.38 ± 0.2	68.8 ± 3.8	286.5 ± 1.6	559.1 ± 46.5

Inactivation time constants (τ_1 and τ_2) were obtained by curve fitting of the inactivation current to a sum of two exponential functions using Igor Pro 5.02. Recovery from inactivation (τ_{rec}) was analyzed by fitting current to single exponential function using Origin 6.1. *Statistically significant, $P < 0.01$ (*t*-test), different from their own control without KChIP1. Values are mean ± s.e.m. for 6–9 oocytes. WT, wild type.

Ala15, Ile17 and Pro21 of the inactivation peptide of Kv4.3 make hydrophobic contacts with KChIP1 residues, mainly from the two sidewalls of the pocket, whereas Ala14 directly contacts the bottom of the pocket (**Fig. 3a**).

The two conserved residues Gly18 and Pro21 serve as hinge points that allow the N-terminus of Kv4.3 to make two sharp turns, thus resulting in the segment of residues 22–40 anti-parallel to its preceding residues (6–17) bound to the pocket (**Fig. 1c**). This structural feature of the U-shaped peptide suggests that the length of the segment comprising residues 23–40 may be important for maintaining Kv4 inactivation[29], because a shortened peptide would lead to a steric clash of Kv4.3 and KChIP1 owing to the spatial restrictions of this region. In addition to completely covering the proximal N-terminal residues (6–17), residues 23–40 in Kv4.3N also interact with H10 of KChIP1 through hydrophobic contacts and hydrogen bonds. A deletion of H10 in KChIP1 led to the loss of its binding to the T1 domain of Kv4.3 (data not shown), which is in agreement with previous studies that truncation of H10 in KChIP1 abolished its interaction with Kv4.2 (ref. 21).

To determine which residues are critical for the association of the Kv4.3 N-terminal peptide and KChIP1 in the first interface (**Fig. 3a**), we generated mutations in either KChIP1 or Kv4.3N and assessed their ability to bind to their wild-type partners. A single mutation (Y134E) in KChIP1 and a triple mutation (W8E-P10E-A15E) in Kv4.3N disrupted their interactions with Kv4.3N or KChIP1, respectively (**Fig. 3b**), indicating that these residues are critical for mediating interactions in the first interface. Sequence comparison indicated that the N-terminal hydrophobic residues of the Kv4-family are highly conserved across species, suggesting that these residues mediate hydrophobic-hydrophobic interactions (**Fig. 3c**). To further confirm the functional significance of the mutation Y134E mutation of KChIP1 and the triple mutant of Kv4.3, we tested their effects on the modulation of Kv4.3. As expected, coexpression of wild-type Kv4.3 and wild-type KChIP1 resulted in a substantial increase in current intensity, slower inactivation and an accelerated recovery from inactivation, compared to Kv4.3 alone (**Fig. 3d** and **Table 2**). In contrast, the KChIP1 Y134E mutation that abolished its interaction with Kv4.3N did not affect Kv4.3 channel function (**Fig. 3d**). As a control, the KChIP1 L115E mutation,

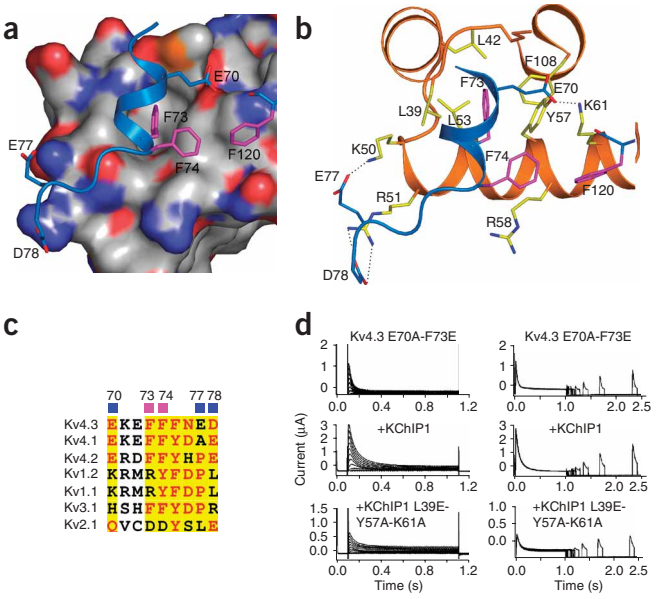

Figure 4 The second contact interface between KChIP1 and Kv4.3 T1 domain. (**a**) The interaction in the second interface is mediated by both hydrophobic contacts and salt bridges. The KChIP1 molecule and Kv4.3 peptide (residues 70–78) are shown in the surface representation and light blue ribbon, respectively. The residues of Kv4.3 that are colored in magenta are involved in hydrophobic interactions with KChIP1. The blue, red and white represent the positive, negative and hydrophobic surface of Kv4.3, respectively. (**b**) A close-up view of the interaction in the second interface between KChIP1 and Kv4.3N. The KChIP1 molecule is shown as a light blue ribbon and the residues involved in the interaction with Kv4.3N are highlighted in yellow. The O and N atoms are shown as red and blue, respectively. The salt bridges are indicated by black dashed dots. (**c**) Sequence alignment of the Kv4.3 peptide (70–78) with the corresponding sequences of other Kv proteins. The residues Phe73 and Phe74 of the Kv4-family are labeled as magenta squares on the top and form hydrophobic contacts with the KChIP1 molecule and those with blue squares make salt bridges with KChIP1. (**d**) The representative traces were recorded from oocytes injected with cRNAs of Kv4.3 double mutant (E70A, F73E) that disrupt the second interface, in the presence or absence of wild-type KChIP1 or the KChIP1 triple mutant (L39E, Y57A, K61A). Left, currents from oocytes held at –80 mV by a family of pulses from –60 to 40 mV in 10 mV increments for 1s. Right, recovery from inactivation for varying lengths of time at step from –80 to 40 mV every 8 s.

which interacts with Kv4.3N (**Fig. 3b**), retained its ability to affect Kv4.3 channels in a manner similar to the wild-type KChIP1 (data not shown). All of these results show that the first interface mediates the functional interaction between Kv4.3 and KChIP1, as disruption of this interface by mutations in either Kv4.3 or KChIP1 resulted in the loss of Kv4.3 modulation by KChIP1. The physical immobilization of the Kv4.3 N-terminal peptide by KChIP1 suggests that the peptide is involved in the inactivation gating, which would provide a structural basis for the elimination of the open-state inactivation of Kv4.3 by KChIP1 (refs. 27,30).

The second interface mediates intersubunit interaction

Besides sequestering the N-terminal peptide of Kv4.3, KChIP1 was unexpectedly shown to interact with a neighboring Kv4.3N, constituting a second interface between them. The interaction around this interface is mainly mediated by H2 of KChIP1 and the Kv4.3 residues 70–78 (**Fig. 4a**,**b**). In the second interface, Phe73 was conserved among the Kv4 members, but not among the other Kv channels (**Fig. 4c**), and it fits tightly into a hydrophobic cavity that is formed by the residues Leu39, Leu42, Leu53, Tyr57 and Phe108 in KChIP1 (**Fig. 4a**,**b**). In addition to the hydrophobic interactions, salt bridges also seem to be important in the interactions in the second interface. Two consecutive acidic residues, Glu77 and Asp78 from Kv4.3N, form salt bridges with residues Lys50 and Arg51 of KChIP1, respectively (**Fig. 4b**). Glu70, another conserved residue among the Kv4 members (**Fig. 4c**), also makes a salt bridge with Lys61 in KChIP1 (**Fig. 4b**). This basic residue is conserved among the KChIPs, but not in other EF-hand proteins such frequenin and recoverin, suggesting a function for salt bridges in the specific recognition of Kv4 by KChIPs.

To assess the functional significance of the residues that are crucial for the interaction in the second interface, we generated a double mutant of Kv4.3, E70A-F73E, and examined its modulation by KChIP1. Alone, this double mutation yielded functional channels, although it had faster inactivation kinetics than wild-type Kv4.3 (**Fig. 4d** and **Table 2**). When coexpressed with the Kv4.3 double mutant, wild-type KChIP1 increased the current amplitude by about threefold and slowed the fast time constant of inactivation, but had only a slight effect on the slow time constant of inactivation and little effect on the recovery from inactivation, compared with the double mutant alone (**Fig. 4d** and **Table 2**). In contrast, when the Kv4.3 double mutant was coexpressed with the KChIP1 triple mutant (L39E-Y57A-K61A), the increase seen with the Kv4.3 double mutant was completely abolished, compared with the effect of wild-type KChIP1 on the Kv4.3 double mutant (**Fig. 4d**). Both the double mutation of Kv4.3 and the triple mutation of KChIP1 in the second interface retained the KChIP1 modulation of inactivation, but not of current amplitude, suggesting that the second interface functions in the surface expression of the channel. These results also indicate that the disruption of either interface can result in a loss of Kv4.3 modulation by KChIP1 (**Figs. 3** and **4**), suggesting that the two interfaces act in concert to facilitate the proper assembly of the channel complexes.

Stabilization of Kv4.3 tetramer by KChIP1

In the clamping mode of the complex, KChIP1 can be depicted as a clamp that holds two Kv4.3 molecules firmly together (**Fig. 1c**,**d**). Thus, we can expect a more stable tetrameric Kv4.3 to be formed by KChIP1 binding. Indeed, it has been shown that KChIP3 can rescue the Zn^{2+} mutant that disrupts the tetramerization of Kv4.2, which strongly suggests that KChIP3 is important for stabilizing Kv4.2 channel assembly[17]. If the tetramer of Kv4.3 is in fact strengthened by the binding of KChIP1, then disruption of the interaction at either of the interfaces will eliminate this stabilizing effect. To confirm this, we examined the ability of the KChIP1 triple mutant L39E-57A-K61A to rescue the tetramerization of the Zn^{2+} mutant (C110A) of Kv4.3N using a gel-filtration assay. As expected, a higher fraction of this Zn^{2+} T1 mutant was eluted as a monomer at low molecular weights (**Fig. 5a**) and the gel showed a significant shift to the tetramer after the addition of wild-type KChIP1 (**Fig. 5a**). In contrast, the C110A mutant of Kv4.3 remained as a monomer with almost no shift to the tetramer after the addition of the KChIP1 triple mutant (**Fig. 5b**), although it retained its ability to interact with the wild-type Kv4.3N, because of the intact first interface (data not shown). These results indicate that the association of KChIP1 with Kv4.3N in the second interface is important in stabilizing the tetramer of Kv4.3.

To further confirm the function of the second interface in stabilizing the Kv4.3 tetramer, we used the electrophysiological assay to test whether the KChIP1 triple mutant can rescue the Kv4.3 C110A mutant. Consistent with previous observations[17], the Kv4.3 C110A mutant alone did not express a functional A-type current (**Fig. 5c**), and coexpression of wild-type KChIP1 rescued the function of the mutant with increased current amplitude, characteristic A-type gating kinetics and a faster recovery from inactivation (**Fig. 5c**). In contrast, coexpression of the KChIP triple mutant only rescued limited functions of the Kv4.3 C110A mutant, with a small increase of the current

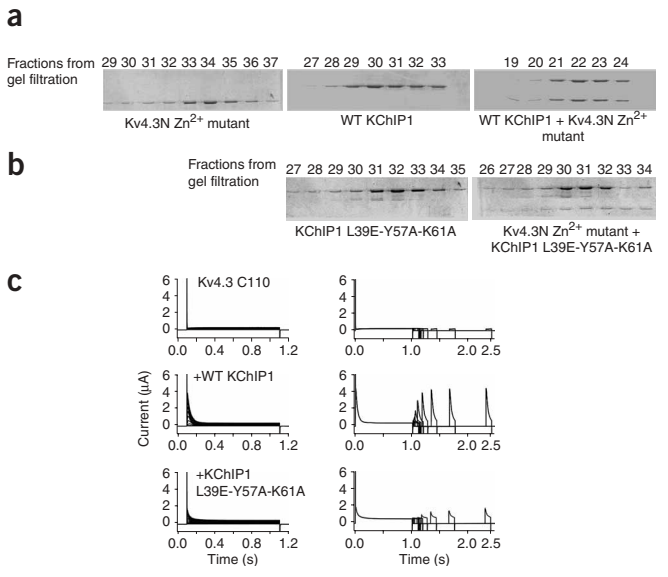

Figure 5 Disruption of the second interface by KChIP1 mutation failed to rescue the tetrameric mutant of Kv4.3 C110a mutant that destabilizes tetrameric assembly. (**a**) The gel bands show the molecular size of protein fractions collected for the tetrameric Kv4.3 C110a mutant, wild-type (WT) KChIP1 and the complex between them. Proteins from each fraction were detected by Coomassie staining after SDS-PAGE. The Kv4.3 mutant was eluted at the monomer position (left) and shifted to the tetramer position (right) when complexed with WT KChIP1. (**b**) The KChIP1 triple mutant at the second interface lost its ability to rescue the tetrameric Kv4.3 C110A mutant. The triple mutant of KChIP1 (L39E, Y57A, K61A) formed a complex with the Kv4.3 C110A mutant owing to the existence of the first interface, but this complex was much smaller than the one formed between WT KChIP1 and the same Kv4.3 mutant, as it was eluted in the 30–32 fractions. (**c**) The triple mutant of KChIP1 (L39E, Y57A, K61A) at the second interface could not rescue the functional expression of the Kv4.3 C110A mutant that disrupts T1 domain interaction and tetrameric assembly. The triple mutant of KChIP1 had no effect on the recovery from the inactivation of the Kv4.3 C110A mutant.

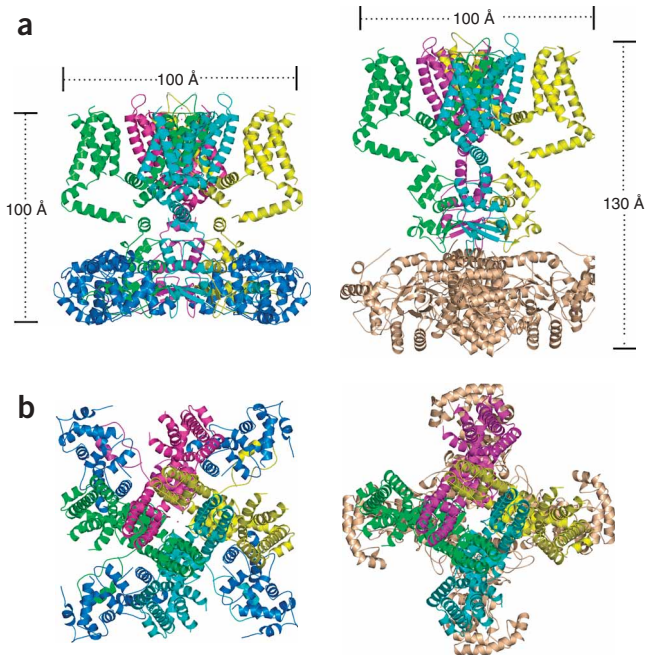

Figure 6 Comparison of the modeled Kv4.3-KChIP1 channel complex with Kv1.2-Kvβ2. (**a**) Side views of Kv1.2–Kv4.3 T1-KChIP complex in which the Kv4.3 T1 domain fused with transmembrane-spanning domains of Kv1.2 (left) and Kv1.2-Kvβ2 complex (right). The tetrameric subunits of Kv1.2 channels are labeled in cyan, yellow, pink and green, respectively. KChIP1 and Kvβ2 are labeled in blue and wheat, respectively. (**b**) Top views of **a**, showing KChIPs positioned between two adjacent T1 domains (left) and Kvβ2 beneath the T1 domains (right).

amplitude, but no recovery of inactivation, compared with the coexpression of wild-type KChIP1 with the Kv4.3 C110A mutant (**Fig. 5c** and **Table 2**). This suggests that these KChIP1 residues from the second interface are important in promoting the tetrameric assembly of functional channels. These functional tests, coupled with the results of the gel-filtration assay, suggest that one of the functions of KChIPs binding to Kv4 proteins is to stabilize the channel complex and thus promote their tetrameric assembly or trafficking to the membrane surface[17]. This notion of a molecular clamp may present a unique mechanism by which KChIP proteins regulate the current density of Kv4 channels through the second interface, which is in contrast to known α-β interactions, such as Kv1.2/Kvβ2, in which Kvβ2, itself as a tetramer, may function by stabilizing channel assembly and promoting the surface expression of Kv1.2 (refs. 31–33). Therefore, it will be interesting to determine whether tetramerization of Kvβ2 is required for its function in augmenting the surface expression of Kv1.2.

Structural comparison of Kv4.3N-KChIP and Kvα-Kvβ complexes

The crystal structures of Kv4.3 and the Kv1.2 T1 domain show a marked similarity, with an r.m.s. deviation of 1.05 Å over the aligned Cα atoms, although their sequences share only 24.6% identity. The tetramers assembled from two distinct T1 domains of Kv4.3 and Kv1.2 also resemble each other. The fact that the membrane-spanning domains of the two channel proteins have a much higher sequence identity (46.0%) suggests that the overall architectures of Kv4.3 and Kv1.2 are similar. We therefore modeled the Kv4.3-KChIP1 channel complex, using the transmembrane segments of Kv1.2 for the modeling and then compared it with the Kv1.2-Kvβ complex[33]. KChIP1 laterally attaches two Kv4.3 N-termini (**Fig. 6a,b**). In contrast, Kvβ2 is immediately underneath one T1 domain, aligning well with the Kv1.2 tetramer and resulting in a substantial increase in the height of the Kv1.2-Kvβ channel complex (**Fig. 6a**). By residing between two adjacent T1 domains, KChIP1 firmly fortifies the Kv4.3 tetramer so that the binding of KChIP1 to the T1 domain essentially does not change the height of the Kv4.3 channel (**Fig. 6a,b**), which is consistent with the EM structure of the Kv4.2-KChIP2 complex[22].

Summary

The modulation of pore-forming α-subunits by their auxiliary subunits remains a central theme for understanding the native channel complex and defining the molecular mechanisms that underlie this process is of great importance. In the present study, we solved the structure of the Kv4.3N and KChIP1 complex. The co-crystal structure reveals a precise organization of KChIP1 binding to Kv4N. In this clamping mode of KChIPs and Kv4 interaction, the fact that one KChIP molecule binds as a monomer (not a dimer) to two adjacent N-termini of Kv4 indicates that there are two contact interfaces, which provides a framework for the structural basis of the interaction by which KChIPs modulate Kv4 function. The first contact interface involves the physical binding and immobilization of the hydrophobic N-terminal peptide of Kv4 channels by KChIPs, resulting in changes of gating kinetics and possibly the efficient trafficking of the channel. The second interface, formed between the same KChIP1 molecule and an adjacent N-terminal domain of Kv4.3, acts in concert with the first one to stabilize the tetramerization of Kv4.3 channels. It is also noteworthy that the mechanism of Kv4 modulation is complex, as other auxiliary proteins like DPPX or other regions of the channel, such as the C-terminus, are also involved in this process. Nonetheless, the clamping mode presented here may serve as a basis for understanding the functions of other KChIP subunits. In addition, the identification of the key interacting residues has implications for the structure-based design of therapeutic chemical compounds for specifically disrupting the interaction.

METHODS

Molecular biology and materials. All materials not specifically identified were purchased from Sigma. All of the PCR reactions were performed using Pfu DNA Polymerase (Stratagene) and the inserts were completely verified by sequencing. The DNA used for yeast transformations and mammalian transfections was purified by affinity columns (Qiagen). All restriction enzymes were purchased from New England Biolabs, Inc. Human Kv4.3 and KChIP1 cDNAs were amplified from brain libraries by PCR using the QuikChange II mutagenesis kit (Stratagene). Inserts of all of the clones and mutants were rigorously verified by sequencing.

Two-electrode voltage clamp recording in *Xenopus laevis* oocytes. For oocyte expression, wild-type or mutant Kv4.3 and KChIP1 cDNAs were subcloned into pBluescript KSM (Neuron 04). The cRNAs were then *in vitro* transcribed using the T3 mMESSAGE Machine kit (Ambion) after the linearization of the cDNA construct with *Not*I. *Xenopus* oocytes (stage V–VI) were selected and injected with 46 nl of solution, containing 0.5–4.0 ng of the selected cRNA, using a microinjector (Drummond Scientific Co.). One to two days after injection, oocytes were impaled with two microelectrodes (0.5–1.0 MΩ) filled with 3 M KCl in a 40-μl recording chamber. The chamber was constantly perfused with ND-96 recording solution, containing 96 mM NaCl, 2 mM KCl, 1 mM $MgCl_2$, 1.0 mM $CaCl_2$ and 5 mM HEPES, pH 7.6. Currents were recorded in ND-96 using a GeneClamp 500 amplifier (Axon Instruments). All recordings were conducted at room temperature (22 ± 1 °C). Data was acquired and analyzed using Pulse software (HEKA). Data, low-pass filtered at 200 Hz, was digitized at 1.0 kHz using an ITC-16 interface (Instrutech Corp.) and analyzed using PulseFit (HEKA Electronics), Igor (Wave Metrics) or Microcal Origin 6.1 (OriginLab). Inactivation time constants (τ_1 and τ_2) were obtained by fitting double exponential functions to the decaying phases of Kv4.2 currents. The

inactivation time constant τ_1 was defined as the predominant component of current amplitude. The activation or kinetics of the recovery from inactivation were analyzed by curve fitting current to a single exponential function. All data are given as mean ± s.e.m. and statistical significance was assessed by *t*-test.

Protein expression and purification. Human Kv4.3 and KChIP1 cDNAs were subcloned into prokaryotic expression vectors for protein production. KChIP1 (residues 38–217) and the Kv4.3 cytoplasmic N-terminus (residues 6–145) were subcloned into pET28a (Novagen) and pGEX-2T (Pharmacia), respectively, and were coexpressed in *Escherichia coli* strain BL21 (DE3). Cells expressing Kv4.3 and KChIP1 were inducted with 1 mM IPTG for 8 hours at room temperature, pelleted, then resuspended in buffer A (50 mM Tris pH 8.0, 100 mM NaCl) and supplemented with 1 tablet per 20 ml of buffer A of Complete EDTA-free protease inhibitors (Roche) using 5 ml of buffer A per gram of cell pellet. The cells were lysed by sonication and then centrifuged at 14,000 RPM for 1.0 hour. The soluble fraction of the complex was purified using GST4B resin and further cleaned by the use of an anion-exchange column (Source-15Q, Pharmacia) and gel filtration chromatography (Superdex200, Pharmacia). Recombinant KChIP1 and the T1 domain of Kv4.3 were over-expressed and purified as described[19].

***In vitro* interaction assay.** Proteins used for interaction assays were cloned into the bacterial expression vectors pGEX-6P1 and PET-30a. To test the interaction between wild-type KChIP1 and mutants of Kv4.3 (residues 6–145), we bound ~100 μg of the various mutant proteins, fused with glutathione S-transferase (GST), to glutathione agarose beads and ~300 μg of histidine (His)-tagged KChIP1 were allowed to flow through the beads. After extensive washing with a buffer containing 25 mM Tris (pH 8.0), 100 mM NaCl and 3.0 mM dithiothreitol (DTT), the bound proteins were visualized by SDS-PAGE with Coomassie blue staining. To examine the interaction of KChIP1 mutants with Kv4.3, we bound ~100 μg of wild-type His-tagged wild-type KV4.3 (residues 6–245) to nickel (Ni) resin and ~300 μg of various KChIP1 mutants (purified by a glutathione–Sepharose 4B affinity column and removal of the GST) were allowed to flow through the Ni resin. After extensive washing with a buffer containing 25 mM Tris (pH 8.0) and 100 mM NaCl, the bound proteins were visualized by SDS-PAGE with Coomassie staining.

Crystallization and data collection. Crystallization conditions for the KChIP1-Kv4.3N complex were determined from the sparse matrix screen (Hampton Research). Screening was done with hanging-drop vapor diffusion by combining 1 μl of protein solution (about 10 mg ml^{-1} in 10 mM Tris, pH 8.0, 100 mM NaCl and 3.0 mM DTT) with 1 μl of well solution at 23.0 °C. Small, pyramid-like crystals appeared overnight in a mother liquor consisting of 2.0 M NaH_2PO_4, 2.0 M K_2HPO_4, 0.2 M Li_2SO_4 and 0.1 M CAPS, pH 10.5. Conditions were further optimized by reducing the phosphate salt concentration to 1.4–1.5 M. Crystals grew to their maximum size (0.15 × 0.15 × 0.1 mm^3) in approximately 1 week. The crystals were transferred to mother liquor with 25% glycerol added, and then flash cooled in liquid nitrogen. A single crystal, diffracting to 3.2 Å, was used for the data collection at beam line F1 in the Cornell High Energy Synchrotron Source, using a Quantum 4 CCD detector. All the data were integrated with DENZO and then scaled and merged with SCALEPACK[34]. The crystal belongs to space group *I*222 (a = 112.186, b = 112.213Å, c = 141.051Å) and contains two KChIP-Kv4.3 complexes per asymmetric unit.

Structure determination and refinement for KChIP1-Kv4.3 complex. The KCHIP1-Kv4.3 crystal structure was determined by molecular replacement (AMORE, included in CCP4)[35] using the coordinates of Kv4.3 and the T1 domain of Kv4.3 as the searching models, respectively. The solutions for KChIP1 and T1 domain of Kv4.3 were combined to form the two complexes in one asymmetric unit for subsequent refinement. Structural refinement was carried out using the program CNS[36]. The initial molecular model included the residues of KChIP1 and the T1 domain without the inactivation peptide of Kv4.3. The model was refined against 20–3.2-Å X-ray data. The progress of the refinement was monitored with the electron density maps and the values of the crystallographic *R*-factors. The electron density for the N-terminal peptide of Kv4.3 became obvious after the preliminary refinement of the model. The residues from the N-terminal inactivation peptide of Kv4.3 were built into the electron density with program O[36] and further refined by position refinement. The final model contains 5,116 protein atoms, 4 Ca^{2+} and 2 Zn^{2+} and corresponds to the R_{work} = 0.258 and R_{free} = 0.302 using the data from 20–3.2 Å.

Accession codes. The atomic coordinates for the Kv4.3N-terminus and KChIP1 complex have been deposited at the Protein Database Bank under the accession code 2NZ0 and will be released upon the publication of this manuscript.

ACKNOWLEDGMENTS

We thank V.J. Karplus for helpful comments on this manuscript and P. Liang for technical support. K.W.W. thanks J. S. Han, Y. Wan and C. Zhou for their support, and specially thanks J. M. Wang for her consistent support and understanding. This work was supported by the '985' grant from the Chinese Ministry of Education and the grant for Project 30630017 by the National Science Foundation of China to K.W.W. and the '863' grant (2003-AA210090) from the Chinese Ministry of Science and Technology to J.J.C. The crystallographic data were collected at the Cornell High Energy Synchrotron Source, which is supported by the National Science Foundation and the National Institute of Health under awards DMR-0225180 and RR01646.

AUTHOR CONTRIBUTIONS

H.W. performed the structural biochemistry experiments and Y.Y. conducted the electrophysiology and part of the molecular biology experiments. Q.L., Q.Y. and Q.H. collected the structural data. Y.H, Y.C. and L.C. provided support in for the molecular biology experiments. Y.C. provided electrophysiology support. K.W.W. and J.C. designed and supervised the experiments and wrote the manuscript.

COMPETING INTERESTS STATEMENT

The authors declare that they have no competing financial interests.

Published online at http://www.nature.com/natureneuroscience
Reprints and permissions information is available online at http://npg.nature.com/reprintsandpermissions/

1. Abbott, G.W. & Goldstein, S.A. A superfamily of small potassium channel subunits: form and function of the MinK-related peptides (MiRPs). *Q. Rev. Biophys.* **31**, 357–398 (1998).
2. Trimmer, J.S. Regulation of ion channel expression by cytoplasmic subunits. *Curr. Opin. Neurobiol.* **8**, 370–374 (1998).
3. Shibata, R. *et al.* A fundamental role for KChIPs in determining the molecular properties and trafficking of Kv4.2 potassium channels. *J. Biol. Chem.* **278**, 36445–36454 (2003).
4. Birnbaum, S.G. *et al.* Structure and function of Kv4-family transient potassium channels. *Physiol. Rev.* **84**, 803–833 (2004).
5. Rhodes, K.J. *et al.* KChIPs and Kv4 alpha subunits as integral components of A-type potassium channels in mammalian brain. *J. Neurosci.* **24**, 7903–7915 (2004).
6. An, W.F. *et al.* Modulation of A-type potassium channels by a family of calcium sensors. *Nature* **403**, 553–556 (2000).
7. Kuo, H.C. *et al.* A defect in the Kv channel-interacting protein 2 (KChIP2) gene leads to a complete loss of I(to) and confers susceptibility to ventricular tachycardia. *Cell* **107**, 801–813 (2001).
8. Holmqvist, M.H. *et al.* Elimination of fast inactivation in Kv4 A-type potassium channels by an auxiliary subunit domain. *Proc. Natl. Acad. Sci. USA* **99**, 1035–1040 (2002).
9. Nadal, M.S. *et al.* The CD26-related dipeptidyl aminopeptidase-like protein DPPX is a critical component of neuronal A-type K^+ channels. *Neuron* **37**, 449–461 (2003).
10. Connor, J.A. & Stevens, C.F. Voltage clamp studies of a transient outward membrane current in gastropod neural somata. *J. Physiol. (Lond.)* **213**, 21–30 (1971).
11. Sheng, M., Tsaur, M.L., Jan, Y.N. & Jan, L.Y. Subcellular segregation of two A-type K^+ channel proteins in rat central neurons. *Neuron* **9**, 271–284 (1992).
12. Serodio, P., Vega-Saenz de Miera, E. & Rudy, B. Cloning of a novel component of A-type K^+ channels operating at subthreshold potentials with unique expression in heart and brain. *J. Neurophysiol.* **75**, 2174–2179 (1996).
13. Johnston, D. *et al.* Dendritic potassium channels in hippocampal pyramidal neurons. *J. Physiol. (Lond.)* **525**, 75–81 (2000).
14. Malin, S.A. & Nerbonne, J.M. Elimination of the fast transient in superior cervical ganglion neurons with expression of KV4.2W362F: molecular dissection of IA. *J. Neurosci.* **20**, 5191–5199 (2000).
15. Shibata, R. *et al.* A-type K^+ current mediated by the Kv4 channel regulates the generation of action potential in developing cerebellar granule cells. *J. Neurosci.* **20**, 4145–4155 (2000).
16. Schoppa, N.E. & Westbrook, G.L. Regulation of synaptic timing in the olfactory bulb by an A-type potassium current. *Nat. Neurosci.* **2**, 1106–1113 (1999).
17. Kunjilwar, K., Strang, C., DeRubeis, D. & Pfaffinger, P.J. KChIP3 rescues the functional expression of Shal channel tetramerization mutants. *J. Biol. Chem.* **279**, 54542–54551 (2004).
18. Jahng, A.W. *et al.* Zinc mediates assembly of the T1 domain of the voltage-gated K channel 4.2. *J. Biol. Chem.* **277**, 47885–47890 (2002).

19. Scannevin, R.H. *et al.* Two N-terminal domains of Kv4 K^+ channels regulate binding to and modulation by KChIP1. *Neuron* **41**, 587–598 (2004).
20. Li, M., Jan, Y.N. & Jan, L.Y. Specification of subunit assembly by the hydrophilic amino-terminal domain of the Shaker potassium channel. *Science* **257**, 1225–1230 (1992).
21. Zhou, W., Qian, Y., Kunjilwar, K., Pfaffinger, P.J. & Choe, S. Structural insights into the functional interaction of KChIP1 with Shal-type K^+ channels. *Neuron* **41**, 573–586 (2004).
22. Kim, L.A. *et al.* Three-dimensional structure of I(to); Kv4.2-KChIP2 ion channels by electron microscopy at 21 Angstrom resolution. *Neuron* **41**, 513–519 (2004).
23. Gulbis, J.M., Zhou, M., Mann, S. & MacKinnon, R. Structure of the cytoplasmic beta subunit-T1 assembly of voltage-dependent K^+ channels. *Science* **289**, 123–127 (2000).
24. Orlova, E.V., Papakosta, M., Booy, F.P., van Heel, M. & Dolly, J.O. Voltage-gated K^+ channel from mammalian brain: 3D structure at 18A of the complete (alpha)4(beta)4 complex. *J. Mol. Biol.* **326**, 1005–1012 (2003).
25. Jerng, H.H. & Covarrubias, M.K. K^+ channel inactivation mediated by the concerted action of the cytoplasmic N- and C-terminal domains. *Biophys. J.* **72**, 163–174 (1997).
26. Jerng, H.H., Shahidullah, M. & Covarrubias, M. Inactivation gating of Kv4 potassium channels: molecular interactions involving the inner vestibule of the pore. *J. Gen. Physiol.* **113**, 641–660 (1999).
27. Gebauer, M. *et al.* N-type inactivation features of Kv4.2 channel gating. *Biophys. J.* **86**, 210–223 (2004).
28. Lewit-Bentley, A. & Rety, S. EF-hand calcium-binding proteins. *Curr. Opin. Struct. Biol.* **10**, 637–643 (2000).
29. Baldwin, T.J., Tsaur, M.L., Lopez, G.A., Jan, Y.N. & Jan, L.Y. Characterization of a mammalian cDNA for an inactivating voltage-sensitive K^+ channel. *Neuron* **7**, 471–483 (1991).
30. Beck, E.J., Bowlby, M., An, W.F., Rhodes, K.J. & Covarrubias, M. Remodelling inactivation gating of Kv4 channels by KChIP1, a small-molecular-weight calcium-binding protein. *J. Physiol. (Lond.)* **538**, 691–706 (2002).
31. Shi, G. *et al.* Beta subunits promote K^+ channel surface expression through effects early in biosynthesis. *Neuron* **16**, 843–852 (1996).
32. Gulbis, J.M., Mann, S. & MacKinnon, R. Structure of a voltage-dependent K+ channel beta subunit. *Cell* **97**, 943–952 (1999).
33. Long, S.B., Campbell, E.B. & Mackinnon, R. Crystal structure of a mammalian voltage-dependent Shaker family K^+ channel. *Science* **309**, 897–903 (2005).
34. Otwinowski, Z. & Minor, W. Processing of X-ray diffraction data collected in oscillation mode. in *Methods in Enzymology*, 307–326 (eds. Carter Jr., C.W. & Sweet, R.M.) (Academic Press, New York, 1997).
35. CCP4 (Collaborative Computational Project 4). The CCP4 suite programs for protein crystallography. *Acta Crystallogr. D* **50**, 760–763 (1994).
36. Brunger, A.T. *et al.* Crystallography & NMR system: a new software suite for macromolecular structure determination. *Acta Crystallogr. D Biol. Crystallogr.* **54**, 905–921 (1998).